Soft Matter

Accepted Manuscript

ROYAL SOCIETY OF CHEMISTRY

www.rsc.org/softmatter

The coexisting phase behavior of thermo-responsive copolymer solutions

Chao Feng[†],Chun-lai Ren[†,*] and Yu-qiang Ma[†,‡,*]

[†] *National Laboratory of Solid State Microstructures and Department of Physics, Nanjing University, Nanjing 210093, China*

‡ *Center for Soft Condensed Matter Physics and Interdisciplinary Research, Soochow University, Suzhou 215006, China*

Abstract

Using a molecular theory for dilute PEO-b-PNIPAm solutions, we first take the formation of hydrogen bonds between copolymer monomers and water molecules into account, which enables us to study the impact of temperature on PEO-b-PNIPAm self-assembly effectively by quantitatively describing the different change of water affinities of two blocks. With the increase of temperature, hydrogen bonds between PNIPAm and water break down dramatically, resulting in the hydrophobic character of PNIPAm while PEO remains hydrophilic. Amphiphilic copolymers in the aqueous surrounding can aggregate into various structures: micelle and vesicle. According to the equilibrium criterion of the excess grand potential under the condition of the grand canonical ensemble, we find both structures are stable and can coexist. Theoretically calculated potentials of mean force of aggregates further verify the coexistence of micelle and vesicle, although the low critical solution temperatures of different aggregates are different under this circumstance. Phase diagram as functions of temperature and the weight fraction of PEO (f_{PEO}) is obtained, which shows different regions of micelle, vesicle and their coexistence. It implies the appearance of two types of micelle-vesicle transition: spontaneous and temperature-induced. Since PEO-b-PNIPAm as a thermoresponsive material has a broad range of applications, a systematical investigation of the phase behavior is very useful not only for the scientific interests but also for the practical applications.

I. INTRODUCTION

Much attention has been paid on stimuli-responsive materials, since the responsive properties are relevant to many biotechnological and biomedical applications.[1] One essential character of these materials is that they can undergo dramatic changes of physicochemical properties in accord with small variations in the environmental conditions, such as changes in pH, ionic strength, and temperature.[2–8] Poly(ethylene oxide)-block-poly(N-isopropylacrylamide)(PEO-b-PNIPAm) block copolymer is one of the famous thermo-responsive materials for the critical temperature around the temperature of human body and the reversible self-assembling behavior. It is soluble in aqueous environment when temperature is low. As the temperature is increased, PNIPAm becomes hydrophobic and the phase separation shows the low critical solution temperature (LCST). Above LCST, copolymers form aggregates. Interestingly, there are rich structures of PEO-b-PNIPAm aggregates. Generally speaking, nanoscaled micelle and vesicle structures are two categories. Tenhu and co-workers studied the aggregation of PEO-b-PNIPAm in water by fluorescence spectroscopy and light scattering. They reported that the shape and size of the aggregates are tunable.[9] It implies PEO-b-PNIPAm may be a good candidate as the carrier for drug delivery systems. On the other hand, some literatures pointed out the possible coexistence of different aggregates,[10–12] and others observed the micelle-vesicle transition under different conditions.[13–16] Obviously, a rich phase behavior is one of the important characters of PEO-b-PNIPAm. However, systematic experimental studies of PEO-b-PNIPAm phase behavior are rare. In this respect it is necessary to clarify the phase behavior of PEO-b-PNIPAm solutions before a wide variety of applications.

In the perspective of theoretical modelings, several works based on the mean-field approximation[10,17,18] have been proposed to study the phase behavior of the copolymer solutions. It has been verified that micelle and vesicle can coexist in binary copolymer mixtures.[10] Unfortunately, most of these works focused on the structures of copolymer aggregates at fixed temperatures. Changes on the structures aroused by the continuous change of temperature have not been accomplished. One challenge in the modelling is how to describe the change of intermolecular interactions between water molecules and copolymer monomers due to the change of temperature. This is important because solvent affinities of each of the blocks are significantly different as temperature is changed. A previous

work[10] using Flory-Huggins parameters to reflect the effective interactions between solvent and different copolymer blocks, which is not enough to describe the thermo-responsive polymer systems because of lacking a clear relationship between temperature and effective interactions. Another challenge is how to reflect the conformational change of copolymers trigged by elevated temperature. Within the frame of the mean-field approaches, the way to overcame the challenges is to include as much molecular detail on intra and intermolecular interactions as possible since the end structure of stimuli-responsive polymer systems is dictated by a subtle interplay among all kinds of interactions and the conformational entropy of macromolecules.

In the present paper, we use a molecular theory to study the self-assembly of PEO-b-PNIPAm solutions. The theory was previously used to study the thermodynamics and structural properties of tethered polymers[19,20] with the consideration of the conformation, size, and shape of each molecule, and was shown to be in quantitative agreement with simulations and experimental observations.[21–23] Recently, the theory has been extended to explicitly include hydrogen bonds between polymers and solvent,[24,25] where the polymer solubility depending on temperature was well established. We aim to model the thermo-responsive behavior of PEO-b-PNIPAm by including different abilities of two blocks to form hydrogen bonds with water. Since the free energy aroused by hydrogen bonding is a function of temperature, it makes us possible to study the change of structures of PEO-b-PNIPAm aggregates induced by the continuous change of temperature. Here we focus on the stability of different aggregates. Thermodynamic criteria is used to verify the coexistence of micelle and versicle. Furthermore, a phase diagram as functions of temperature and the weight fraction of PEO is given, providing a comprehensive investigation of the self-assembly of the dilute PEO-b-PNIPAm solutions.

The paper is organized as follows. First, we describe the molecular theory, focusing on the formulism of hydrogen bonds between copolymer monomers and solvents. Second, we present relevant results, concentrating on the stability and LCST of PEO-b-PNIPAm aggregates. Moreover, a phase diagram is obtained. At last, we draw a conclusion on the self-assembly of PEO-b-PNIPAm solutions and discuss some possible reasons in experiments that may lead to the deviation of end-state structures from equilibrium states.

II. MODEL AND THEORY

Systems interested here are PEO-b-PNIPAm solutions. Our purpose is the systematic study on the self-assembly of PEO-b-PNIPAm under the influence of temperature and the weight fraction of PEO. We consider only the case of dilute solutions where interactions between aggregates are ignored. Although there are different shapes of aggregates depending on the length of different blocks, here we just take the spherical aggregates into account for simplicity. The extension to other geometries is straightforward but beyond the scope of the present work. We use spherical coordinates where r denotes the radial distance from the center of the aggregate. The Helmholtz free energy of the aggregate is given by:

$$\beta F = -\frac{S_p}{k_B} + \beta F_{inter} - \frac{S_w}{k_B} + \beta U_{rep} + \beta F_{hb} \tag{1}$$

where $\beta = 1/k_B T$ is the inverse absolute temperature.

The first term in Eq.(1) is the entropy of copolymer chains, which is written as:

$$\frac{-S_p}{k_B} = \int \rho_p(r)[\sum_{\beta_r} P(\beta_r)\ln P(\beta_r) + \ln \rho_p(r) v_w - 1]4\pi r^2 dr \tag{2}$$

where $\rho_p(r)$ is the density of copolymer and $P(\beta_r)$ is the the probability distribution function (pdf) of finding a chain in conformation β with the first segment at r. Eq.(2) accounts for both conformational entropy and translational entropy of copolymers in the aggregate.

The second term of Eq.(1) represents the effective intermolecular interactions between different species, which is

$$\beta F_{inter} = \int [\frac{\chi_{we}}{v_w}\langle\phi_e(r)\rangle\phi_w(r) + \frac{\chi_{wn}(r)}{v_w}\langle\phi_n(r)\rangle\phi_w(r) + \frac{\chi_{en}}{v_w}\langle\phi_e(r)\rangle\ \langle\phi_n(r)\rangle]4\pi r^2 dr \tag{3}$$

where $\chi_{we}, \chi_{wn}, \chi_{en}$ describe the strength of the water-PEO, water-PNIPAm, PEO-PNIPAm effective repulsions. First two Flory-Huggins parameters determine the quality of the solvent in the absence of hydrogen bonds, and the last reflects the different chemical character between two blocks. $\langle\phi_i(r)\rangle$ represents the average volume fraction of monomers of type i ($i = e$ PEO and $i = n$ PNIPAm) at distance r from the center of the aggregate, and it is given by

$$\langle\phi_i(r)\rangle = \frac{\int \rho_p(r^{'})\sum_{\beta_{r^{'}}} P(\beta_{r^{'}})[n_i(\beta_{r^{'}}, r)dr]v_i 4\pi r^{'2} dr^{'}}{4\pi r^2 dr} \tag{4}$$

where $n(\beta_{r^{'}}, r)dr$ is the number of segments for a copolymer chain in conformation β with the first segment at $r^{'}$ attributed to the spherical layer from r to $r + dr$. v_i is the volume

of each segment of type i. The water volume fraction is given by $\phi_w(r) = \rho_w(r)v_w$, with the density of water molecules $\rho_w(r)$ in the layer between r and $r + dr$.

The third term in free energy expression is the translational (mixing) entropy of water molecules, which is given by

$$-\frac{S_w}{k_B} = \int \rho_w(r)[\ln \rho_w(r)v_w - 1]4\pi r^2 dr \tag{5}$$

The fourth term in Eq. (1) represents the excluded-volume repulse interactions between all the molecules, which is in the form of

$$\beta U_{rep} = \int \beta\pi(r)[\langle\phi_e(r)\rangle + \langle\phi_n(r)\rangle + \phi_w(r) - 1]4\pi r^2 dr \tag{6}$$

where $\pi(r)$ represents the distance-dependent repulsive interaction field, which basically is a Lagrange multiplier ensuring the incompressibility of the system. The packing constraint of the whole system is

$$< \phi_e(r) > + < \phi_n(r) > +\phi_w(r) = 1. \tag{7}$$

The last term in the expression of the free energy aroused by the formation of hydrogen bonds between different segment and water, and water molecules themselves, which is given by

$$\begin{aligned}\beta F_{hb} \;=\; & \sum_j \int 2\rho_j(r)[x_{wj}(r)\ln x_{wj}(r) + (1 - x_{wj}(r))\ln(1 - x_{wj}(r)) - x_{wj}(r)\beta\Delta F_{wj}]4\pi r^2 dr \\ & + \int 2\rho_w(r)[1 - \sum_j \frac{x_{wj}(r)\rho_j(r)}{\rho_w(r)}]\ln[1 - \sum_j \frac{x_{wj}(r)\rho_j(r)}{\rho_w(r)}]4\pi r^2 dr \\ & - \int 2\rho_w(r)[\sum_j \frac{x_{wj}(r)\rho_j(r)}{\rho_w(r)}]\ln\frac{2\rho_w(r)v_w}{e}4\pi r^2 dr\end{aligned} \tag{8}$$

with $j = e, n, w$ reflecting hydrogen bonds between water and different species.

The derivation of the different terms in Eq.(8) were discussed in our previous works[24,25] inspired by the work of Dormidontova.[26] Here we point out their origins considering the possibility of water-water, water-PEO and water-PNIPAm binding and take into account that water can work as both hydrogen bond acceptor and donor while the PEO and PNIPAm segments only serve as hydrogen bond acceptors. $\rho_j(r)$ is the number density of segments of type j and $x_{wj}(r)$ denotes the fraction of hydrogen bonds between donor provided by water and acceptor j. ΔF_{wj} is the intrinsic free energy of a single hydrogen bond, including

the energetic gain and entropic loss: $\beta\Delta F_{wj} = \beta\Delta E_{wj} - \Delta S_{wj}/k_B$ with $\Delta S_{wj} = -\ln((1 - \cos\Delta_{wj})/2)$. It should be noted that the intrinsic free energy of hydrogen bonding depends on temperature, which implies the formation of hydrogen bonds controlled by temperature. It is the competition between the different types of hydrogen bonds resulting in the amphiphilic character of PEO-PNIPAm above LCST. The intrinsic free energy of water-water and water-PEO hydrogen bonding is chosen as previous works.[24–26] $\Delta E_{ww}/k_B$ and $\Delta E_{we}/k_B$ are fixed as 1800 K and 2000 K respectively. Δ_{ww} and Δ_{we} equal to $\pi/4.75$ and $\pi/8.35$. According to the data reported by Dixon *et al.*[27], we choose $\Delta E_{wn}/k_B = 2300K$ for the water-PNIPAm binding, and $\Delta_{wn} = \pi/18.45$ based on simulations done by Netz *et al.*[28]. Therefore, for a certain temperature, ΔF_{we} is larger than ΔF_{wn}, indicating the association of water-PEO is more favorable than the binding of water-PNIPAm. Moreover, water-PEO hydrogen bonds become more prevailing with the increase of temperature.

The Helmholtz free energy given by Eq. (1) is useful for a closed system with fixed numbers of molecules. However, in order to determine the phase behavior of PEO-PNIPAm solution, we need to consider an open system where molecules are exchangeable inside and outside the aggregate. This is accomplished by constructing a grand canonical system. The grand potential of the system is

$$\beta W = \beta F - \int 4\pi r^2[\rho_p(r)\beta\mu_p + \rho_w(r)\beta\mu_w]dr \tag{9}$$

Here we consider copolymer and water can be exchanged with the fixed chemical potentials μ_p and μ_w.

To find equilibrium solutions, we minimize the grand potential with respect to different variables. It turns out that the probability distribution function $P(\beta_r)$ is expressed as:

$$\begin{aligned} P(\beta_r) = \frac{1}{q_{\beta_r}} \exp\{ & -\int \beta\pi(r')[n_e(\beta_r, r')v_e + n_n(\beta_r, r')v_n]dr' - \\ & \int 2dr'\{n_e(\beta_r, r')\ln[1 - x_{we}(r')] + n_n(\beta_r, r')\ln[1 - x_{wn}(r')]\} - \\ & \int dr'[\frac{\chi_{wn}(r')}{v_w} n_n(\beta_r, r')v_n\phi_w(r') + \frac{\partial\chi_{wn}(r')}{v_w\partial\phi_n(r')} n_n(\beta_r, r')v_n\langle\phi_n(r')\rangle\phi_w(r') + \\ & \frac{\chi_{we}}{v_w} n_e(\beta_r, r')v_e\phi_w(r') + \frac{\chi_{en}}{v_w} n_e(\beta_r, r')v_e\langle\phi_n(r')\rangle + \frac{\chi_{en}}{v_w}\phi_e(r')n_n(\beta_r, r')v_n]\} \end{aligned} \tag{10}$$

The volume fraction of water is given by:

$$\begin{aligned} \phi_w(r) = \exp[& \beta\mu_w - \beta\pi(r)v_w - \chi_{we}\langle\phi_e(r)\rangle - \chi_{wn}(r)\langle\phi_n(r)\rangle - 2\ln(1 - x_{ww}(r)) - \\ & 2\ln(1 - x_{ww}(r) - \frac{x_{we}(r)\rho_e(r)}{\rho_w(r)} - \frac{x_{wn}(r)\rho_n(r)}{\rho_w(r)})] \end{aligned} \tag{11}$$

The density of copolymers is:

$$\rho_p(r)v_w = q_{\beta_r} \exp[\beta\mu_p] \tag{12}$$

Fractions of different types of hydrogen bonds are:

$$\ln x_{wj}(r) - \ln(1 - x_{wj}(r)) - \beta\Delta F_{wj} = \ln 2\rho_w(r)v_w + \ln[1 - \sum_j \frac{x_{wj}(r)\rho_j(r)}{\rho_w(r)}] \tag{13}$$

with $j = e, n$, and w.

Important to note that the system can be viewed as the aggregate immersing in the bulk solution, where copolymers are free and hydrogen bonds between different species still exist. So that the chemical potentials of the molecules can be calculated from the bulk. We can write down the free energy for bulk, which looks like Eq. (9) except all the variables are not position dependent anymore and they are constant due to the homogeneous bulk system. After minimization, we can get:

$$\beta\mu_w = \ln\phi_w^b + \chi_{we}^b\phi_e^b + \chi_{wn}^b\phi_n^b + 2\ln(1 - x_{ww}^b) + 2\ln(1 - x_{ww}^b - \frac{x_{we}^b\rho_e^b}{\rho_w^b} - \frac{x_{wn}^b\rho_n^b}{\rho_w^b})] \tag{14}$$

$$\beta\mu_p = \ln\frac{\rho_p^b v_w}{q_\alpha^b} \tag{15}$$

$$\ln x_{wj}^b - \ln(1 - x_{wj}^b) - \beta\Delta F_{wj} = \ln 2\rho_w^b v_w + \ln[1 - \sum_j \frac{x_{wj}^b\rho_j^b}{\rho_w^b}] \tag{16}$$

with $j = e, n$, and w. Here the superscript of 'b' is assigned to be the bulk. With the input of bulk concentration, fractions of hydrogen bonds and chemical potentials are known.

Thus, the unknowns in above equations are the position dependent repulsive fields and fractions of hydrogen bonds. These quantities are determined by substituting Eqs. (10)-(13) into the packing constraint Eq.(7). In practice, we convert the integral equations into a set of coupled nonlinear equations by discretizing the space, while details on the discretization, numerical methodology and how the chains are generated can be found in the Appendix.

III. RESULTS AND DISCUSSIONS

In this section, we will present relevant results. Before showing the results, we should comment on the choice of parameters used in all the calculations. In order to get a proper quan-

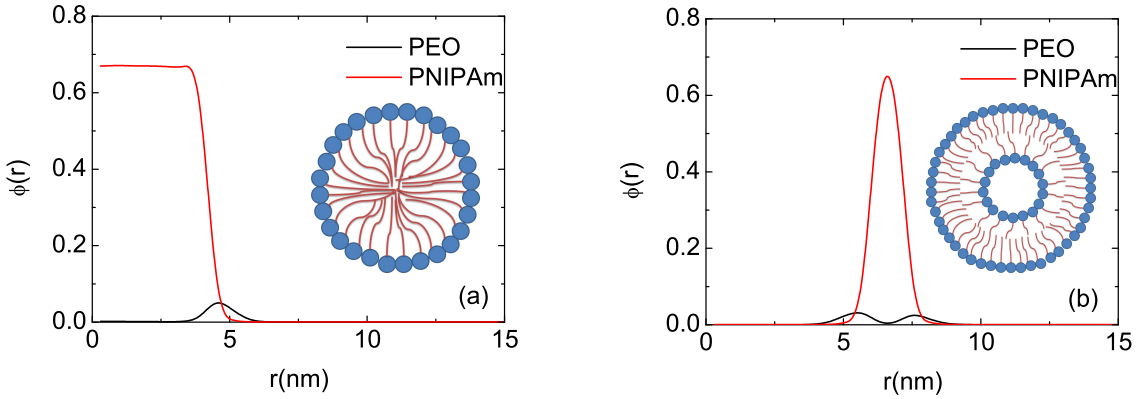

FIG. 1: The volume fraction profiles of PNIPAm and PEO as a function of distance from the center of (a)micelle and (b)vesicle. The insets are schemas of micelle and vesicle, respectively. Black lines correspond to the volume fraction of PEO, and red lines are the volume fraction of PNIPAm. The distributions are calculated according to the experimental condition[9] with the temperature $T = 38^oC$, the weight fraction of PEO $f_{PEO} = 0.077$, and the concentration of bulk solution $\rho_{bulk} = 2.3 * 10^{-4}M$.

titative theoretical evaluation compared with experimental data, Flory-Huggins parameters are introduced to describe the complicated interactions in such multi-component system. The effective interaction between water and PEO χ_{we} is chosen of the form $\chi_{we} = B/T$, with $B = 100K$. Here we do not include an entropic-dependent term, as is done in general.[24,26] χ_{wn} is chosen as what Afroze et al did in their experimental fitting,[29] which is complex because it also reflects the association among PNIPAm monomers with the increase of temperature. χ_{en} is fixed as a small constant just for the chemical difference between two blocks of the copolymer. The polymerisation of PEO-b-PNIPAm is fixed as 23 throughout this paper for the following two reasons. First, we intend to obtain the nano-scaled aggregates, which require short chain length of copolymers, as Li *et al.*[10,30] did in their works. Second, we assume all the aggregates are spherical. Numerical results show us that short copolymers prefer to form the spherical aggregate.

In our numerical calculations, we use different initial guesses and get non-trivial self-consistent solutions, implying different structures of PEO-b-PNIPAm aggregates shown in Fig. 1. The origin of X axis represents the center of aggregates. Fig. 1(a) shows the micelle structure with the core of PNIPAm and the shell of PEO. Fig. 1(b) presents the vesicle

structure with PNIPAm inside and PEO outside the bilayer. It should be mentioned that the calculations were carried on in the grand canonical ensemble, which means the number of copolymers in aggregates are not fixed. Chemical potentials of copolymer in different types of aggregates are same to the one of free copolymer in bulk solution determined by the bulk concentration. It is important to note the aggregation number N_{agg} of copolymers in aggregates, which directly relates to the size of aggregates. Using the formula of $N_{agg} = \int(\rho_p(r) - \rho_{bulk})4\pi r^2 dr$, we find the aggregation number of micelle $N_m = 69$ and vesicle $N_v = 153$. From Fig. 1, we also can see the radius of the micelle is around $5nm$ and that of vesicle is about $8nm$. One interesting thing is that although differences on aggregation number and size are distinct for two types of aggregates, the maximum volume fractions of PNIPAm in Fig. 1(a) and (b) are similar at $\phi_{max} = 0.68$. It means the extent of the molecular packing within aggregates is similar. If they are used as drug carriers, it implies that they have the similar permeability for drug particles passing in and out. This special feature relates to their coexistence as we will show in the following.

The appearance of aggregates is at the temperature higher than LCST. Here we try to use a thermodynamic quantity to capture the appearance of phase transition. According to the Gibbs-Duhem relationship[10], we get the aggregation number of the aggregate $N_{agg} = -(\frac{\partial \epsilon}{\partial \mu_p})_{\mu_w}$, where the excess grand potential of aggregate, $\beta\epsilon = \beta W - \beta W_{bulk}$, reflects the excess free energy for the formation of aggregate. For a stable aggregate at the temperature higher than LCST, the aggregation number N_{agg} is necessarily positive, which means that the excess grand potential should be a decreasing function of the chemical potential of copolymer. It is the case that Fig. 2(b) and (d) present. On the other hand, $\beta\epsilon$ keeps at zero when the temperature is lower than LCST, shown by Fig. 2(a) and (c). Therefore, LCST of micelle is 36^oC and that of vesicle is 38^oC for dilute the PEO-b-PNIPAm solution with the weight fraction of PEO $f_{PEO} = 0.077$. The difference on LCST for different aggregates originates in the molecular character, i. e., the ratio of PEO and PNIPAm. It determines the inherent geometry during the formation of the aggregate in the aqueous surrounding. As temperature is increased above LCST, hydrogen bonds between water and copolymer monomers tend to break down further, which in turn makes PEO-b-PNIPAm molecules more flexible and helps the formation of different structures. The excess grand potential of aggregate can also be defined as $\epsilon = N_{agg} f$, where f is the excess free energy per molecule of forming the aggregate. Although the excess grand potentials of micelle and

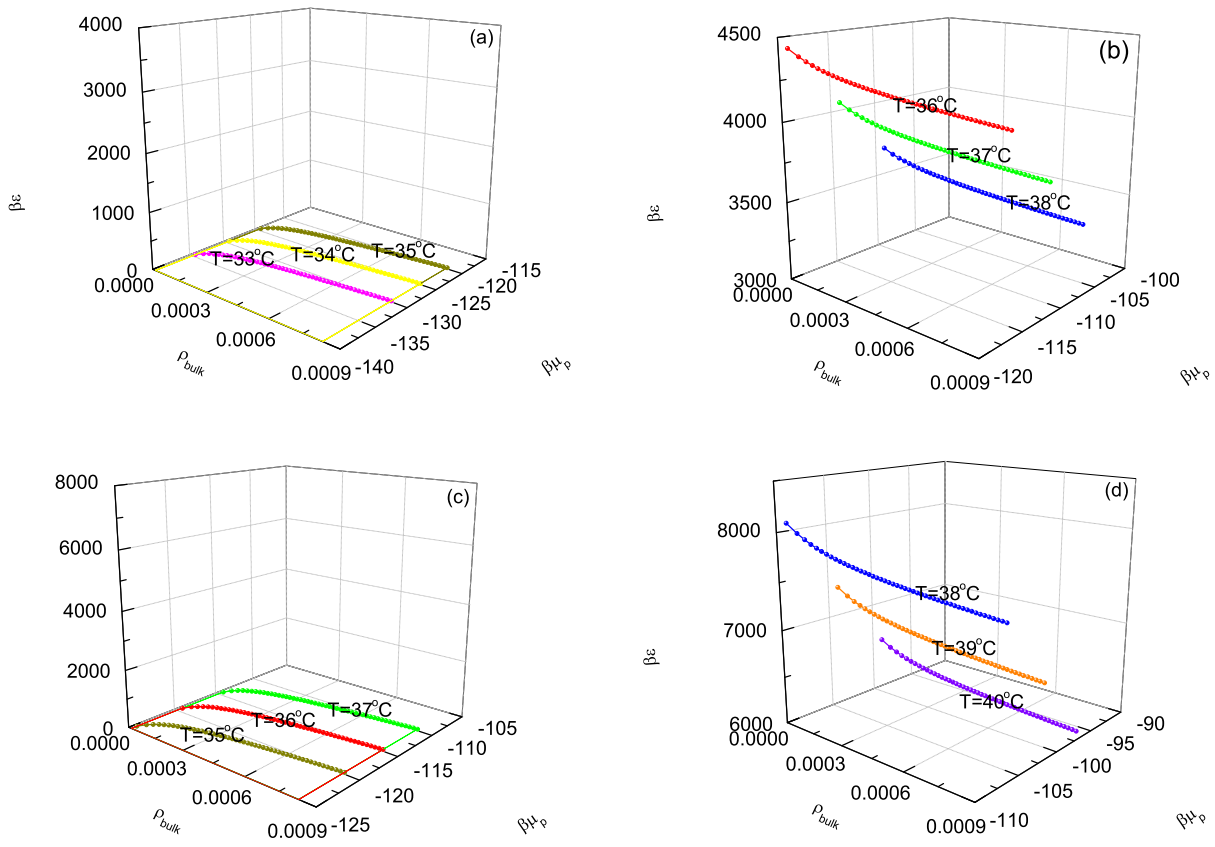

FIG. 2: The excess grand potential as functions of the bulk concentration and the chemical potential of copolymer for two aggregates with different temperatures. Temperatures lower (a) and higher (b) than the LCST of micelle. Temperatures lower (c) and higher (d) than the LCST of vesicle.

vesicle are very different, $\epsilon_m = 3491.7 k_B T$ and $\epsilon_v = 7656.6 k_B T$, the excess free energies per molecule for these two structures are very similar: $f_m = 50.6 k_B T$ and $f_v = 50.0 k_B T$. The negligible difference on the free energy per molecule, less than $1 k_B T$, implies the possibility of the coexistence between micelle and vesicle.

The existence of LCST is the sign of PEO-b-PNIPAm changing from water soluble molecule to amphiphilic copolymer. To quantify this change, we turn to fractions of hydrogen bonds between water and two blocks of the copolymer. To better visualize the change on the solvent affinity of two blocks, we draw the difference of hydrogen bond fractions, that is, $\Delta x_{ij} = x_{ij}^{38^oC} - x_{ij}^{35^oC}$. Owing to $T = 35^oC$ lower than LCST, PEO-b-PNIPAm is water soluble with high values of $x_{we}^{35^oC}$ and $x_{wn}^{35^oC}$. With the increase of temperature, hydrogen bond fractions decrease reflected by the negative values of Δx_{we} and Δx_{wn}. The

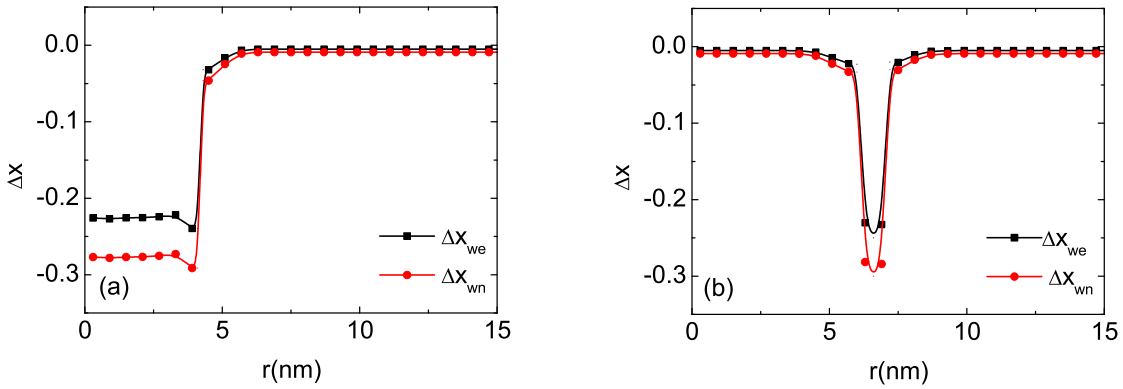

FIG. 3: The differences of hydrogen bond fractions as a function of distance from the center of aggregates: (a)micelle and (b)vesicle. The black line with squares and the red line with cycles correspond to the difference of the hydrogen bond fractions of water-PEO and water-PNIPAm. Parameters are same to Fig.1.

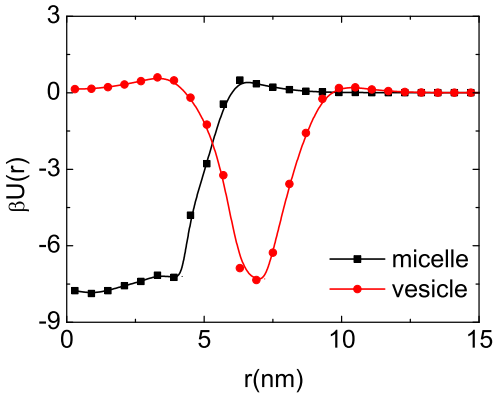

FIG. 4: The potential of mean force for micelle and vesicle as a function of the distance from the center. The black line with squares and the red line with cycles correspond to micelle and vesicle respectively. Parameters are same to Fig.1.

decrease is significant inside of aggregates, as both Fig. 3(a) and (b) show. Furthermore, water-PNIPAm hydrogen bonds break down more than water-PEO bonds, originating from the weaker intrinsic free energy of hydrogen bonding between water and PNIPAm. It is the reason that PEO-b-PNIPAM is thermo-responsive amphiphilic copolymer.

To further verify the inherence of the micelle-vesicle coexistence, it is instructive to look at the expression of the copolymer chemical potential. For the aggregate it is given by

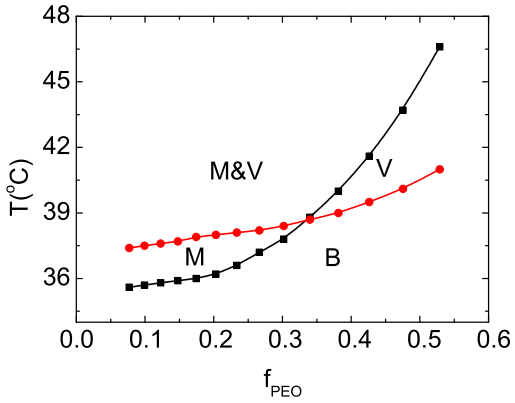

FIG. 5: Phase diagram of PEO-b-PNIPAm solutions as functions of the weight fraction of PEO and temperature at the bulk concentration of $\rho_b = 2.5 * 10^{-4} M$. B represents the homogeneous bulk solution. M reflects the micelle structure. V is the vesicle structure. M & V indicates the coexistence region of micelle and vesicle. Lines with squares and circles represent the LCST of PEO-b-PNIPAm solutions with the formation of micelle and vesicle respectively.

$\beta\mu_p(r) = \ln \rho_p(r) + \beta U(r)$. While for the bulk solution, it is $\beta\mu_p^b$. For the equilibrium, however, the copolymer chemical potential of aggregate is equal to that of the bulk solution. Therefore, the physical meaning of $\beta U(r)$ is the work required to bring a copolymer from the bulk solution to the aggregate at the position of r, which is called the potential of mean force. From our theory $\beta U(r)$ is equal to $-\ln q_{\beta_r}$. This quantity reflects the potential felt by the copolymer in such environmental condition including all the effective interactions between the copolymer and other molecules in the system. It is known that free PEO-b-PNIPAm molecules in the bulk would aggregate when temperature is increased above LCST. Meanwhile they feel the steric repulsion during the course of aggregation due to local crowding. All these factors compete resulting in the final aggregate with the specific structure, size and aggregation number. Although Fig. 4 shows different shapes of $\beta U(r)$ for micelle and vesicle, an important common feature is that both cases have the similar minimum about $U_{min} = -7.5 k_B T$ residing at the most condensed inner of aggregates. This implies that the similar driving forces result in the micelle and vesicle structures. The coexistence of micelle and vesicle is proved.

So far we have discussed the effect of temperature on the self-assembly of PEO-b-PNIPAm solutions. Another important factor is the weight fraction of PEO,[31] which basically deter-

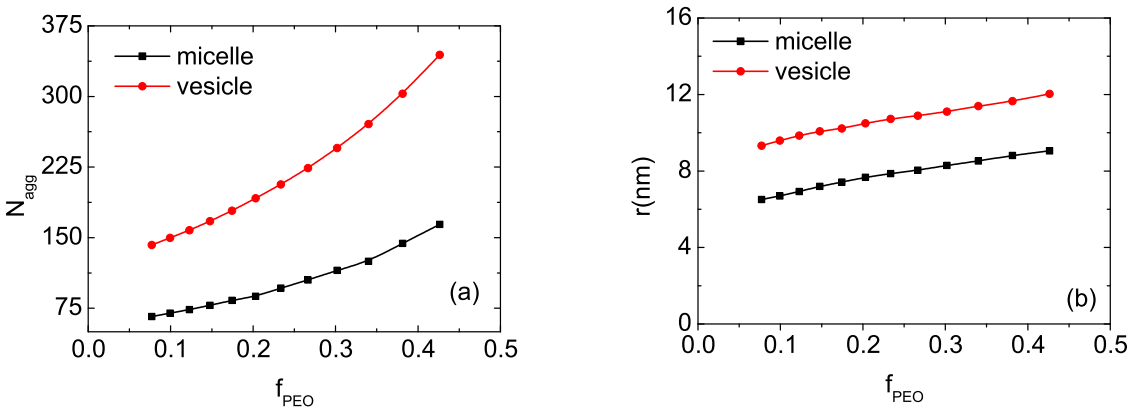

FIG. 6: (a)Aggregation number (b) the radius of aggregates as a function of weight fraction of PEO for PEO-b-PNIPAm solution with the bulk concentration of $\rho_b = 2.5 * 10^{-4}M$ and at the temperature of $T = 42^oC$. Lines with squares and circles represent micelles and vesicles respectively.

mines the proportion of hydrophilic and hydrophobic part of the copolymer. Fig. 5 provides the phase diagram of dilute PEO-b-PNIPAm solutions. The border between the bulk and the solution with micelle or vesicle structure is the LCST of the solution. It shows the LCST shifts to higher temperature as the weight fraction of PEO increases, just as many experiments reported.[31,32] It is worth noting that when temperature is a little higher than LCST, PEO-b-PNIPAm aggregates have the specific structure according to f_{PEO}, which relates to the inherent molecular geometry. The coexistence of micelle and vesicle would happen when the temperature is much higher than LCST, where copolymers are more flexible because of less hydrogen bonds with solvents. According to the phase diagram, spontaneous micelle-vesicle transition can happen in the coexistence region, while temperature-induced micelle-vesicle (or vesicle-micelle) transition can be observed for specific PEO-b-PNIPAm solutions when temperature is increased from just above LCST to much higher than LCST. Moreover, all the transitions are reversible.

For the practical applications of nano-sized aggregates, PEO-b-PNIPAm has the advantage of size controllable. Choosing a high temperature at $T = 42^oC$ within the coexistence region in the phase diagram, we intend to see the impact of f_{PEO} on the size of aggregates. Fig. 6 gives the aggregation number and the radius of aggregates changing with f_{PEO}. As the length of PEO-b-PNIPAm is fixed, PNIPAm block becomes shorter and shorter with

the increasing of f_{PEO}. In order to keep similar condensed packing within aggregates, aggregation numbers should be increased, as Fig.6 (a) shows. It, of course, gives rise to the size of aggregates seen in Fig. 6(b). However, N_{agg} shows the nonlinear rising behavior, while r is almost the linear increase. This provides a good guide for the precisely controlling aggregation size.

IV. CONCLUSIONS

We particularly formulate the hydrogen bonds between water-PEO and water-PNIPAm for PEO-b-PNIPAm solutions within the frame of the molecular theory, which makes a systematic study of the self-assembly of thermo-responsive copolymers possible. Fractions of hydrogen bonds between water-PEO and water-PNIPAm quantitatively reflect the amphiphilic character of PEO-b-PNIPAm above LCST. When the temperature is higher than LCST, we find both micelle and vesicle structures are stable according to the criterion of the excess grand potential. The micelle-vesicle coexistence is further proved by the analysis of the potential of mean force of aggregates. A phase diagram as functions of temperature and the weight fraction of PEO is obtained, which shows different regions with different structures, especially a large region of coexistence of micelle and vesicle. It indicates the existing of two types of reversible transition: spontaneous and temperature-induced micelle-vesicle transition.

It should be noted that our study is based on the thermodynamic equilibrium. Although some experiments[11,12] have reported the coexistence of micelle and vesicle in copolymer solutions, the structure of vesicle is not easy to be observed in experimental conditions compared with micelle. One main reason is that the aggregation number of vesicle usually is large, which may lead to a rather long time to achieve the thermal equilibrium state. Therefore, the end state is easily trapped into a nonequilibrium metasable state. On the other hand, the role of kinetics [33] has been reported in many amphiphilic molecules self-assembly systems, which also is an important factor determining the final structure of aggregates. Of course, other factors, such as compositional fluctuations and interactions between aggregates, would affect the final structure of solutions.

With regard to the modelling, this is a successful try for us to quantitatively reflect the copolymer character transforming from soluble to amphiphilic at LCST by introducing hy-

drogen bonds between water and different blocks. It is useful for thermo-responsive systems. Of course, there are many different types of responsive materials intrigued by other stimuli, such as pH, salt, light, and so on. Although various mechanisms are involved, the idea of modeling is similar, including as much detail on intra and intermolecular interactions at the molecular level as possible. At this stage, we always turn to simulations based on the atomic level for much molecular information, then move to the theoretical coarse-grained modelling which enables us to investigate systems in large time and size scales in the comparison of experiments. Therefore, the theoretical modelling works as a bridge linking microscopic simulations and macroscopic experiments.

Acknowledgments. This work is supported by the National Natural Science Foundation of China under Grants 21274062, and 91027040. We are grateful to the high performance computing center of Nanjing University for doing the numerical calculations in this paper on its IBM blade cluster system. C.-L. R. is grateful to Dr. Wen-de Tian for his careful reading of the manuscript.

V. APPENDIX

Here we present an outline of the numerical method used to solve the equations derived from the molecular theory. This is done by dividing the r-axis into parallel spherical layers of thickness δ. Functions are assumed to be constant within a layer; hence integrations can be replaced by summations. The ith layer is defined as the region between $(i-1)\delta \leq r < i\delta$. The packing constraints, Eq. (7), in a discrete form for layer i is:

$$< \phi_e(i) > + < \phi_n(i) > + \phi_w(i) = 1. \tag{17}$$

The volume fraction of PNIPAM and PEO equals

$$< \phi_j(i) >= \frac{\sum_{i'=1}^{i_{max}} \rho_j(i') \sum_{\beta_{i'}} P(\beta_{i'}) n_j(\beta_{i'}, i) v_j dv(i')}{dv(i)} (j = e, n). \tag{18}$$

where $dv(i) = \frac{4}{3}\pi\delta^3[i^3 - (i-1)^3]$ is the volume of ith layer. Here the discretized probability distribution functions $P(\beta_r)$ is

$$\begin{aligned} P(\beta_i) \;=\; & \frac{1}{q_{\beta_i}} \prod_{i'=1}^{i_{max}} \exp\{-\beta\pi(i')[n_e(\beta_i, i')v_e + n_n(\beta_i, i')v_n] - \\ & 2\{n_e(\beta_i, i')\ln[1 - x_{we}(i')] + n_n(\beta_i, i')\ln[1 - x_{wn}(i')]\} - \\ & [\frac{\chi_{wn}(i')}{v_w} n_n(\beta_i, i')v_n\phi_w(i') + \frac{\partial\chi_{wn}(i')}{v_w\partial\phi_n(i')} n_n(\beta_i, i')v_n\langle\phi_n(i')\rangle\phi_w(i') + \\ & \frac{\chi_{we}}{v_w} n_e(\beta_i, i')v_e\phi_w(i') + \frac{\chi_{en}}{v_w} n_e(\beta_i, i')v_e\langle\phi_n(i')\rangle + \frac{\chi_{en}}{v_w}\phi_e(i')n_n(\beta_i, i')v_n]\} \end{aligned} \quad (19)$$

Volume fractions of water is given by:

$$\begin{aligned} \phi_w(i) \;=\; & \exp[\beta\mu_w - \beta\pi(i)v_w - \chi_{we}\langle\phi_e(i)\rangle - \chi_{wn}(i)\langle\phi_n(i)\rangle - 2\ln(1 - x_{ww}(i)) - \\ & 2\ln(1 - x_{ww}(i) - \frac{x_{we}(i)\rho_e(i)}{\rho_w(i)} - \frac{x_{wn}(i)\rho_n(i)}{\rho_w(i)})] \end{aligned} \quad (20)$$

Fractions of hydrogen bonds are:

$$x_{wj}(i) = 2\rho_w(i)v_w(1 - x_{wj}(i))[1 - \sum_j \frac{x_{wj}(i)\rho_j(i)}{\rho_w(i)}]\exp(\beta F_{wj}) \quad (21)$$

with $j = e, n$ and w. These coupled equations are solved self-consistently.

The chain model for PEO-b-PNIPAm is the three-state RIS model[34]. In this model, each bond has three different isoenergetic states. The conformations are generated by a simple sampling method and all the accepted conformations are self-avoiding. We generate 10^5 independent conformations with the first segment at the first layer, and then transfer them to every layer throughout the system. In our calculations, we divide r into n=50 layers, and thus there are 5×10^6 different conformations for PEO-b-PNIPAm. The same set of conformations has been used in all the calculations presented in this paper. Each segment of PNIPAM has the volume of $v_n = 0.16\ nm^3$,which was chosen according to the partial specific volume of PNIPAM in water,[35] and for PEO and water are $v_e = 0.065\ nm^3$,$v_w = 0.03\ nm^3$ as we use before[24,36]. The layer thickness was $\sigma = 0.6nm$. The interaction parameter $\chi_{wn}(i) = (g_{00} + g_{02}T) + (g_{10} + g_{12}T)\phi_n(i) + (g_{20} + g_{22}T)\phi_n^2$ between water and PNIPAM comes from the experiment of Afroze et al[29], where g_{ij} (i,j=0, 1, 2) are constants.

[1] M. A. C. Stuart, W. T. S. Huck, J. Genzer, M. Mueller, C. Ober, M. Stamm, G. B. Sukhorukov, I. Szleifer, V. V. Tsukruk, M. Urban, F. Winnik, S. Zauscher, I. Luzinov and S. Minko, *Nature*

Materials, 2010, **9**, 101–113.

[2] Y. Qiu and K. Park, *Advanced Drug Delivery Reviews*, 2001, **53**, 321–339.

[3] M. E. Byrne, K. Park and N. A. Peppas, *Advanced Drug Delivery Reviews*, 2002, **54**, 149–161.

[4] T. Miyata, T. Uragami and K. Nakamae, *Advanced Drug Delivery Reviews*, 2002, **54**, 79–98.

[5] D. Schmaljohann, *Advanced Drug Delivery Reviews*, 2006, **58**, 1655–1670.

[6] A. K. Bajpai, S. K. Shukla, S. Bhanu and S. Kankane, *Progress In Polymer Science*, 2008, **33**, 1088–1118.

[7] C. He, S. W. Kim and D. S. Lee, *Journal of Controlled Release*, 2008, **127**, 189–207.

[8] F. Meng, Z. Zhong and J. Feijen, *Biomacromolecules*, 2009, **10**, 197–209.

[9] J. Zhao, G. Zhang and S. Pispas, *Journal of Polymer Science Part A-polymer Chemistry*, 2009, **47**, 4099–4110.

[10] F. Li, A. T. M. Marcelis, E. J. R. Sudholter, M. A. C. Stuart and F. A. M. Leermakers, *Soft Matter*, 2009, **5**, 4173–4184.

[11] Y. Y. Won, A. K. Brannan, H. T. Davis and F. S. Bates, *Journal of Physical Chemistry B*, 2002, **106**, 3354–3364.

[12] F. Zhao, J. Sun, Z. Liu, L. Feng and J. Hu, *Journal of Polymer Science Part B-polymer Physics*, 2010, **48**, 364–371.

[13] T. S. Davies, A. M. Ketner and S. R. Raghavan, *Journal of the American Chemical Society*, 2006, **128**, 6669–6675.

[14] M. Mao, J. B. Huang, B. Y. Zhu and J. P. Ye, *Journal of Physical Chemistry B*, 2002, **106**, 219–225.

[15] A. Mohanty, T. Patra and J. Dey, *Journal of Physical Chemistry B*, 2007, **111**, 7155–7159.

[16] Y. Yang, J. Dong and X. Li, *Journal of Colloid and Interface Science*, 2012, **380**, 83–89.

[17] J. T. Zhu, Y. Jiang, H. J. Liang and W. Jiang, *Journal of Physical Chemistry B*, 2005, **109**, 8619–8625.

[18] V. G. de Bruijn, L. J. P. van den Broeke, F. A. M. Leermakers and J. T. F. Keurentjes, *Langmuir*, 2002, **18**, 10467–10474.

[19] I. Szleifer and M. A. Carignano, *Advances In Chemical Physics, Vol Xciv*, 1996, **94**, 165–260.

[20] I. Szleifer and M. A. Carignano, *Macromolecular Rapid Communications*, 2000, **21**, 423–448.

[21] M. C. Faure, P. Bassereau, M. A. Carignano, I. Szleifer, Y. Gallot and D. Andelman, *European Physical Journal B*, 1998, **3**, 365–375.

[22] R. Shvartzman-Cohen, E. Nativ-Roth, E. Baskaran, Y. Levi-Kalisman, I. Szleifer and R. Yerushalmi-Rozen, *Journal of the American Chemical Society*, 2004, **126**, 14850–14857.

[23] J. Satulovsky, M. A. Carignano and I. Szleifer, *Proceedings of the National Academy of Sciences of the United States of America*, 2000, **97**, 9037–9041.

[24] C.-l. Ren, R. J. Nap and I. Szleifer, *Journal of Physical Chemistry B*, 2008, **112**, 16238–16248.

[25] R. Shvartzman-Cohen, C.-l. Ren, I. Szleifer and R. Yerushalmi-Rozen, *Soft Matter*, 2009, **5**, 5003–5011.

[26] E. E. Dormidontova, *Macromolecules*, 2002, **35**, 987–1001.

[27] D. A. DIXON, K. D. DOBBS and J. J. VALENTINI, *Journal of Physical Chemistry*, 1994, **98**, 13435–13439.

[28] P. A. Netz and T. Dorfmuller, *Journal of Physical Chemistry B*, 1998, **102**, 4875–4886.

[29] F. Afroze, E. Nies and H. Berghmans, *Journal of Molecular Structure*, 2000, **554**, 55–68.

[30] F. Li, S. Prevost, R. Schweins, A. T. M. Marcelis, F. A. M. Leermakers, M. A. C. Stuart and E. J. R. Sudholter, *Soft Matter*, 2009, **5**, 4169–4172.

[31] S. Qin, Y. Geng, D. E. Discher and S. Yang, *Advanced Materials*, 2006, **18**, 2905–2909.

[32] J. Virtanen, S. Holappa, H. Lemmetyinen and H. Tenhu, *Macromolecules*, 2002, **35**, 4763–4769.

[33] J. Leng, S. U. Egelhaaf and M. E. Cates, *Biophysical Journal*, 2003, **85**, 1624–1646.

[34] C.-l. Ren and Y.-q. Ma, *Soft Matter*, 2011, **7**, 10841–10849.

[35] P. Kujawa and F. M. Winnik, *Macromolecules*, 2001, **34**, 4130–4135.

[36] C.-l. Ren, W.-d. Tian, I. Szleifer and Y.-q. Ma, *Macromolecules*, 2011, **44**, 1719–1727.

A theoretical predication of the micelle-vesicle coexisting of PEO-b-PNIPAm solutions